Original Research

The New Role of *HNF1A-NAS1/miR-214/INHBA* Signaling Axis in Colorectal Cancer

Xuan Zhang[1,†], Tao Wu[1,†], Rujia Qin[2], Xinyi Cai[1], Yongchun Zhou[3], Xiaoxiong Wang[3], Zhongjun Shang[4], Guoyu Li[1], Renfang Yang[1], Chao Dong[5], Jinsha Li[1], Yongping Ren[1], Rong Ding[6,*], Yunfeng Li[1,*]

[1]Department of Colorectal Surgery, Yunnan Cancer Hospital, The Third Affiliated Hospital of Kunming Medical University, 650118 Kunming, Yunnan, China
[2]Department of Head and Neck Tumor Surgery, Yunnan Cancer Hospital, The Third Affiliated Hospital of Kunming Medical University, 650118 Kunming, Yunnan, China
[3]Laboratory of Molecular Diagnosis Center, Yunnan Cancer Hospital, The Third Affiliated Hospital of Kunming Medical University, 650118 Kunming, Yunnan, China
[4]Department of Hospital Affairs, Yunnan Cancer Hospital, The Third Affiliated Hospital of Kunming Medical University, 650118 Kunming, Yunnan, China
[5]Department of Oncology, Yunnan Cancer Hospital, The Third Affiliated Hospital of Kunming Medical University, 650118 Kunming, Yunnan, China
[6]Department of Minimally Invasive Intervention, Yunnan Cancer Hospital, The Third Affiliated Hospital of Kunming Medical University, 650118 Kunming, Yunnan, China
*Correspondence: dingrong2@kmmu.edu.cn (Rong Ding); liyunfeng@kmmu.edu.cn (Yunfeng Li)
†These authors contributed equally.

Abstract

Background: Colorectal cancer (CRC) is the third most common cancer and one of the leading causes of death worldwide. Seriously threatens human life and health. Previous studies have identified that inhibin βA (*INHBA*) could induce tumorgenesis and progression of CRC through the regulation of the TGF-β/Smad signal axis. The abnormal expression of *INHBA* is related to the poor prognosis of patients. The aim of this study was to identify the molecular mechanism of *HNF1A-AS1* and *miR-214* regulating *INHBA* and carcinogenesis through bioinformatics combined with experiments. **Methods**: The expression of *HNF1A-AS1*, *miRNA-214-5p*, *INHBA* in pan-cancer and CRC were investigated in the Cancer Genome Atlas (TCGA). The correlation between *HNF1A-AS1* and immune-related genes or miRNAs was explored via the Gene Expression Profiling Interactive Analysis (GEPIA) and volcano plots, respectively. The association between *HNF1A-AS1* and differentially expressed miRNAs was constructed by TargetScan. The miRDB, miRWalk, and TargetScan databases were utilized to predict the target genes of *hsa-miR-214*. The expression of *INHBA* in tissues and cell lines of CRC was examined by RT-qPCR and western blot assay. **Results**: The *INHBA* and *HNF1A-AS1* expressions were increased in Colon adenocarcinoma (COAD) and Rectum adenocarcinoma (READ) of the TCGA database. *Hsa-miR-214* was relatively less expressed in CRC tissues compared with para-cancer tissues. The expression of *HNF1A-AS1* was negatively correlated with *hsa-miR-214*. *INHBA* was one of the target genes of *hsa-miR-214* based on miRDB, miRWalk, and TargetScan databases. The specific binding sites of INHBA-3'UTR and *miR-214-5p* were identified by starBase. The expression level of *INHBA* was positively correlated with the T stage of tumor and negatively correlated with overall survival (OS) and disease-free survival (DFS) in CRC patients. The results of RT-qPCR and western blot indicated that the expression of *INHBA* in tissues and cell lines in CRC was higher than those in para-carcinoma tissues and normal colon cell lines, respectively. **Conclusions**: These findings suggested that *HNF1A-AS1* and *miRNA-214-5p* were key upstream non-coding RNAs of *INHBA*. The *HNF1A-AS1/miR-214/INHBA* signal axis plays a significant role in the tumorgenesis and progression of CRC. By interfering with *HNF1A-AS1* and *INHBA* genes on HT29 and SW480 cells, it was found that *HNF1A-AS1* and *INHBA* genes may be important target genes in CRC.

Keywords: colorectal cancer; *HNF1A-AS1*; miR-214; *INHBA*; TGF-β/Smad

1. Introduction

Colorectal cancer (CRC) is one of the most common gastrointestinal malignancies. In 2020, the incidence of CRC ranked third and the mortality rate ranked second [1]. In addition, CRC is the third most common cancer in males and the second most common in females, with approximately 1.9 million new cases and 0.9 million deaths in 2020 worldwide [2]. CRC is a heterogeneous disease, regulated by numerous factors and intricate biological process, and its occurrence and developmental mechanism remains to be elucidated [3]. In recent years, epigenetic and transcriptome changes have attracted the attention of researchers due to their significant role in tumor development [4,5].

MiRNA is a noncoding single-stranded RNA (19–25 nt) derived from endogenous hairpin structure transcripts, and is a noncoding small molecular RNA. MiRNAs can induce target gene mRNA degradation or target gene translation inhibition through the 3'UTR region or coding region specific base pairing combination, thus regulating target gene expression at the post-transcriptional level [6,7]. Studies have shown that miRNAs play a crucial role in tumor growth, apoptosis, invasion and metastasis [8]. They restrain the expression of target genes by combining with the translation of target genes, and then participate in the regulation of 30% human protein expression, tumorigenesis, development and metastasis [9]. Long noncoding RNA (LncRNA) also has an important role in the research of human tumors. As a competitive endogenous RNA (ceRNA), LncRNA performs a vital role in tumorgenesis by binding miRNAs to regulate the expression of target genes [10,11].

Inhibin is a homodimer or heterodimer consisting of α, βA and βB subunits, which are called inhibin α (*INHA*), inhibin βA (*INHBA*), and inhibin βB (*INHBB*) subunit gene [12]. *INHBA* gene is located on chromosome 7p15-p14 and consists of two exons [12]. As a member of the transforming growth factor beta (TGF-β) superfamily, *INHBA* gene participates in the occurrence and development of tumors by regulating the TGF-β/Smad signaling pathway. Abnormal expression of the *INHBA* gene is associated with poor prognosis of reproductive cancers [13]. Previous researchers have demonstrated that the *INHBA* gene also promotes the invasion and metastasis of cancers by inducing epithelial-mesenchymal transition (EMT), promoting angiogenesis and changing epigenetic mechanisms [14].

Based on the transcriptome data of 473 colon cancer tissues and 41 adjacent tissues collected in the cancer genome atlas (TCGA) database (https://www.cancer.gov/about-nci/organization/ccg/research/structural-genomics/tcga), our research team found that *INHBA* was highly expressed in cancer tissues, and the expression of *INHBA* significantly positively correlated with the T stage of tumor, that is, the higher the expression level of *INHBA*, the later the T stage of patients. The survival curve analysis of gene expression profiling the interactive analysis (GEPIA) database (http://gepia.cancer-pku.cn/) demonstrated that the expression level of *INHBA* was negatively correlated with the survival rate of colon cancer patients, that is, the higher the expression level of *INHBA*, the lower the survival rate of colon cancer patients. RT-qPCR and western blot tests were performed on 17 clinical tumor tissues and para-cancerous tissues. The results showed that the mRNA and protein levels of *INHBA* were highly expressed in tumors. In addition, immunohistochemical (IHC) staining also demonstrated that *INHBA* protein was brownish yellow, was principally located in the cytoplasm, and had high expression of *INHBA* in cancer tissue. LncRNA *HNF1A* antisense RNA 1 (*HNF1A-AS1*) is a 2.455 kb lncRNA located on chromosome 12q24.31. It is transcribed from the opposite strand of the *HNF1A* gene [15]. Previous studies showed that *HNF1A-AS1* and *miR-214* were closely related to the progression of CRC, and bioinformatics confirmed that *miR-214* specifically targets the 3'UTR of the *INHBA* gene. Further analysis indicated that the expression of *HNF1A-AS1* and *miR-214* was consistent in the TCGA database and experiments. In addition, previous studies have shown that the *INHBA* gene can regulate the TGF-β/Smad signaling pathway and promote the occurrence and development of tumors [16]. Therefore, we hypothesized that *miR-214* regulates the activity of the TGF-β/Smad signal axis by targeting *INHBA*, thereby inhibiting the proliferation and metastasis of CRC.

2. Materials and Methods

2.1 Clinical Samples Collection

We collected 60 pairs of CRC tumor and para-cancer tissues from the Yunnan Cancer Hospital/The Third Affiliated Hospital of Kunming Medical University. The age of the CRC patients ranged from 46 to 69 years, including 31 males and 29 females. Baseline demographic and clinical characteristics of all 60 CRC patients were collected. All tumors and adjacent tissues removed from the patient were immediately placed in liquid nitrogen and transported to the laboratory within 2 hours for storage in a –80 °C degree refrigerator. Written informed consent was obtained from all participants prior to their enrollment in the study. The protocols for the present study were approved by the Medical Institutional and Clinical Research Ethics Committee of the Yunnan Cancer Hospital, the Third Affiliated Hospital of Kunming Medical University (refers to the same entity) in accordance with the "Declaration of Helsinki" on the ethical principles for medical research involving human subjects.

2.2 Analysis of HNF1A-AS1 in Diverse Human Tumor

Previous studies have demonstrated that *HNF1A-AS1* is a potential long noncoding RNA which regulates tumor progression. Using the TCGA database, we analyzed the expression of *HNF1A-AS1* in 33 different tumors and adjacent tissues. In addition, we analyzed the expression of *HNF1A-AS1* in colon cancer and rectal cancer tissues and corresponding para-cancer tissues and its association with overall survival (OS). We further verified differences in *HNF1A-AS1* expression in colon cancer and rectal cancer in relative para-cancer tissues in the two databases.

2.3 Differential Expression of HNF1A-AS1/miRNAs

First, we used the "limma 2.11" R package to analyze the differences in *HNF1A-AS1* expression in 477 tumors and 41 neighboring tissues in the TCGA database. Then, we analyzed *HNF1A-AS1* in 125 immune related genes related to the distribution in the tumor and nearby tissue. Differential screening was set at a threshold for |log2 fold

change (FC)| >1 and a *p* value < 0.05, using a screening of the volcano map. Finally, to determine the correlation between *HNF1A-AS1* and differentially expressed miRNAs, TargetScan was used to predict and construct the correlation.

2.4 Gene Ontology (GO) Analysis

To explore the potential functions of 125 immune-related genes associated with *HNF1A-AS1*, GO (is an internationally standardized classification system of gene functions that provides a dynamically updated and controlled vocabulary to comprehensively describe the properties of genes and gene products in an organism) function and Kyoto Encyclopedia of Genes and Genomes (KEGG) pathway enrichment analyses were performed using the R package 'clusterprofiler' R package. In the analysis results, pathways or functions with a *p* value < 0.05 were considered to be significantly enriched.

2.5 Cell Culture and Cell Transfection

The human normal colon epithelial cell lines (NCM460) and the human colon cancer cell lines (HCT116, HT29, SW480, SW620, and LOVO) were purchased from the Cell Bank of the Chinese Academy of Sciences (Shanghai, China). The NCM460 and HCT116 cells were cultured in the Roswell Park Memorial Institute-1640 (RPMI-1640; MeilunBio, Dalian, China) and Dulbecco's modified Eagle's medium (DMEM; Procell, Wuhan, China). The HT29 and SW480 cells were cultured in L15 media (Leibovitz's L-15; Procell), the SW620 and LOVO cells were cultured in F12K media (Ham's F-12K; Procell). Media were supplemented with 10% fetal bovine serum (FBS; Procell) and 100 µg/mL penicillin-streptomycin solution (Procell). Cells were grown at 37 °C incubator with 5% CO_2/95% air. This procedure was also used for the preparation and transfection of *HNF1A-AS1* shRNA and *INHBA* shRNA.

Using Lenti-Pac™ HIV Expression Packaging Kit (GeneCopoeia, Guangzhou, China), the interference plasmid and over-expression plasmid were transfected into 293T cells with DNA-lipofectamine 2000 reagent (Invitrogen; Carlsbad, CA, USA) The complete medium was changed 8 h after transfection. After 48 h of incubation, the culture supernatant rich in lentivirus particles was collected and stored at –80 °C. Following polybrene™ (Merck KGaA, Darmstadt, Germany)-assisted *HNF1A-AS1* interference of lentivirus for 72 h, 1 µg/mL puromycin was used to screen the transfected positive cells. The medium was changed every 2 days and screening with complete medium was continued for 2 weeks to expand the cell culture. All cell lines were genotyped for identity by Shanghai Biowing Applied Biotechnology Co., Ltd. Mycoplasma Removal Agent (0.02ug /ml,C0288M, Biyuntian, Shanghai, China) was added during the experiment. The cell morphology was observed under the microscope, which was similar to that of the ATCC cell bank. STR identification was performed on the experimental cells.

2.6 3-(4,5)-dimethylthiahiazo (-z-y1)-3,5-di-phenytetrazoliumromide (MTT) Assay

Cell viability was demonstrated by a MTT kit (Solarbio, Beijing, China). After performing various treatments, HT29 and SW-480 cells and their transfection with *HNF1A-AS1* shRNA and *INHBA* shRNA were cultured in 96-well plates for 24, 48, 72 and 96 h, respectively. Fresh media were mixed with MTT solution and serially added into culture plates. 4 h later, dimethyl sulfoxide (Sigma, St. Louis, MO, USA) was added into wells to dissolve formazan. Samples were assessed by microplate reader (Thermo Fisher, New York, NY, USA), and results were obtained by analyzing the output of the wavelength at 490 nm.

2.7 Flow Cytometry Analysis

Cell apoptosis was determined by an Annexin V-fluorescein isothiocyanate (Annexin V-PE; Procell) detection kit (Solarbio). Briefly, cultured cells were digested with trypsin (Thermo Fisher), and suspended in binding buffer (Solarbio). Annexin V-PE (Solarbio) and 7-aminoactinomycin D (7-AAD; Solarbio) were then serially incubated with cells in the dark. Finally, samples were analyzed with a flow cytometer (Thermo Fisher).

2.8 Cell Proliferation Ability Test

In preparation of cell suspension, the cells were digested with 0.25% trypsin and collected, and the cells were resuspended and counted with culture supernatant. The cells were seeded into 96-well plates by 4×10^4 cells, with 5 replicates in each group. A total of four 96-well plates were seeded and returned to the incubator for further culture (measured once at 0 h, 24 h, 48 h, 72 h and 96 h, respectively). CCK8 reagent was diluted with basal medium at 10:1. The 96-well plate was removed to remove the cell supernatant in the culture plate, and 100 µL of diluted CCK8 solution was added to each well, and care was taken not to form bubbles in the wells. A blank control well was set, and 100 µL of diluted CCK8 solution was added to the other 3 wells. The samples were returned to the incubator and incubated for 2 h in darkness. The OD value of each well in the 96-well plate was detected at 450 nm with a microplate reader.

2.9 Transwell Invasion Assay

The invasion of HT29 and SW480 cells and their transfection with *HNF1A-AS1* shRNA and *INHBA* shRNA, respectively, was investigated with transwell chambers with Matrigel (Corning, Madison, NY, USA). Cells were seeded in the upper chambers with FBS-free DMEM or L15 media (Procell). DMEM or L15 media containing 15% FBS (Procell) were added into the lower chambers. After 24 h

of culture, the cell supernatant was discarded and cells were singly incubated with methanol (Sigma) as well as crystal violet (Sigma). Results were analyzed by counting the cell numbers in the lower chambers under a microscope (Nikon, Tokyo, Japan) at a $100\times$ magnification.

2.10 Association between HNF1A-AS1 and Differential miRNAs

The relative expression of miRNAs, which is tightly linked with *HNF1A-AS1,* was detected by RT-qPCR in clinical CRC and para-cancer tissues. Subsequently, the association between differentially expressed miRNAs and *HNF1A-AS1* was analyzed.

2.11 Target Gene Analysis of hsa-miR-214

The miRDB, miRWalk, and TargetScan databases were utilized to predict the target genes of *hsa-miR-214*. RT-qPCR was used to detect the relative expression level of target genes located in the overlapping region. The relative expression levels of *INHBA* in CRC and para-cancer tissues were analyzed from the TCGA database. In addition, the expression of *INHBA* at different stages of CRC and its association with disease-free survival (DFS) and OS were analyzed.

2.12 qRT-PCR

Samples were homogenized with Trizol reagent (Takara, Kyoto, Japan), and total RNA was extracted according to the Trizol kit (Takara) instructions. After quantification by NanoDrop 2000 (Takara), 200 ng total RNA was utilized by the ReverTra Ace qPCR RT Kit (Takara) for reverse transcription according to the instructions. THUNDERBIRD SYBR® qPCR Mix (Takara) was used for quantitative Reverse Transcription Polymerase Chain Reaction (qRT-PCR) analysis. CFX96 Touch Real-Time PCR Detection System (Bio-RAD, Hercules, CA, USA) was used for RT-qPCR. GAPDH was used as an internal reference when determining the contents. Corresponding primer sequences are listed in Table 1.

2.13 Western Blotting

Cell lysis buffer solution was added to the sample, and total protein extract was obtained after repeated suspension and centrifugation at 4 degrees. Protein concentration in the extract was detected by the Bradford method. Sodium dodecyl sulfate polyacrylamide gel electrophoresis (SDS-PAGE) was used for protein electrophoresis, followed by 300 mA constant current for 1 h to transfer the protein onto the PVDF membrane. After sealing, the primary antibody was added and shaken overnight at 4 °C. After washing the membrane, a secondary antibody was added and incubated at 37 °C for 2 h. Then luminous solution was and tablet pressing, exposure and fixing were performed. ImageJ (version 1.8.0, LOCI, University of Wisconsin, Madison, WI, USA) analysis was used to obtain the

Table 1. The primers using in qRT-PCR analysis.

Name	Sequence (5′-3′)
H-mir-214-3p	ACAGCAGGCACAGACAGGCAGT
H-mir-1252-3P	CAAATGAGCTTAATTTCCTTTT
H-mir-7151-3P	CTACAGGCTGGAATGGGCTCA
H-mir-3907	AGGTGCTCCAGGCTGGCTCACA
H-mir-3934-3P	TGCTCAGGTTGCACAGCTGGGA
H-mir-4306	TGGAGAGAAAGGCAGTA
H-mir-3665	AGCAGGTGCGGGGCGGCG
H-mir-1303	TTTAGAGACGGGGTCTTGCTCT
H-mir-4668-5P	GAAAATCCTTTTTGTTTTTCCAG
H-mir-10527-5P	AAAGCAAATGTTGGGTGAACGGC
miR-Reverse primer	GTCGTATCCAGTGCAGGGT
U6 F	CTCGCTTCGGCAGCACA
U6 R	AACGCTTCACGAATTTGCGT
HNF1A-AS1 F	TGATGCTGTTCCTTCTACC
HNF1A-AS1 R	GAGTTTCGTTCTTGTTCCC
GAPDH F	CCCATCACCATCTTCCAGG
GAPDH R	CATCACGCCACAGTTTCCC

qRT-PCR, quantitative Reverse Transcription Polymerase Chain Reaction.

images and determine the integral optical density of protein bands. GAPDH protein was selected as the internal reference.

2.14 Immunohistochemistry Assay

IHC assay was performed according to the previous process. Briefly, paraffin sections were placed at 60 °C for 2 h, then washed with dimethylbenzene solution, ethanol, and TBS in sequence. After the antigen was retrieved with citrate buffer solution, endogenous peroxidase was blocked by 1% hydrogen peroxide. Tissues were incubated with primary antibody overnight at 4 °C. Subsequently, the sections were incubated with HRP-labeled goat anti-rabbit immunoglobulin G (1:100; Abcam). Sections were visualized by diaminobenzidine. The sections were then counterstained with hematoxylin and washed by dimethylbenzene solution and ethanol. Finally, the sections were sealed with neutral balsam. The results of the immunohistochemical staining were analyzed with an optical microscope.

2.15 Statistical Analysis

SPSS 23.0 software (IBM Corp., Armonk, NY, USA) was used for data analysis, and graph pad prism 8.0 software (GraphPad Software, Inc., San Diego, CA, USA) was used for statistical mapping. The measured data was represented by mean $\pm$ standard deviation ($\pm$ s). If the data presented normal distribution, a paired sample *t*-test was used for comparison between two groups, and one-way analysis of variance was used for comparison between multiple groups. If the data was not normal, non-parametric testing was used. Counting data were tested by χ^2 test. $p < 0.05$ was considered statistically significant.
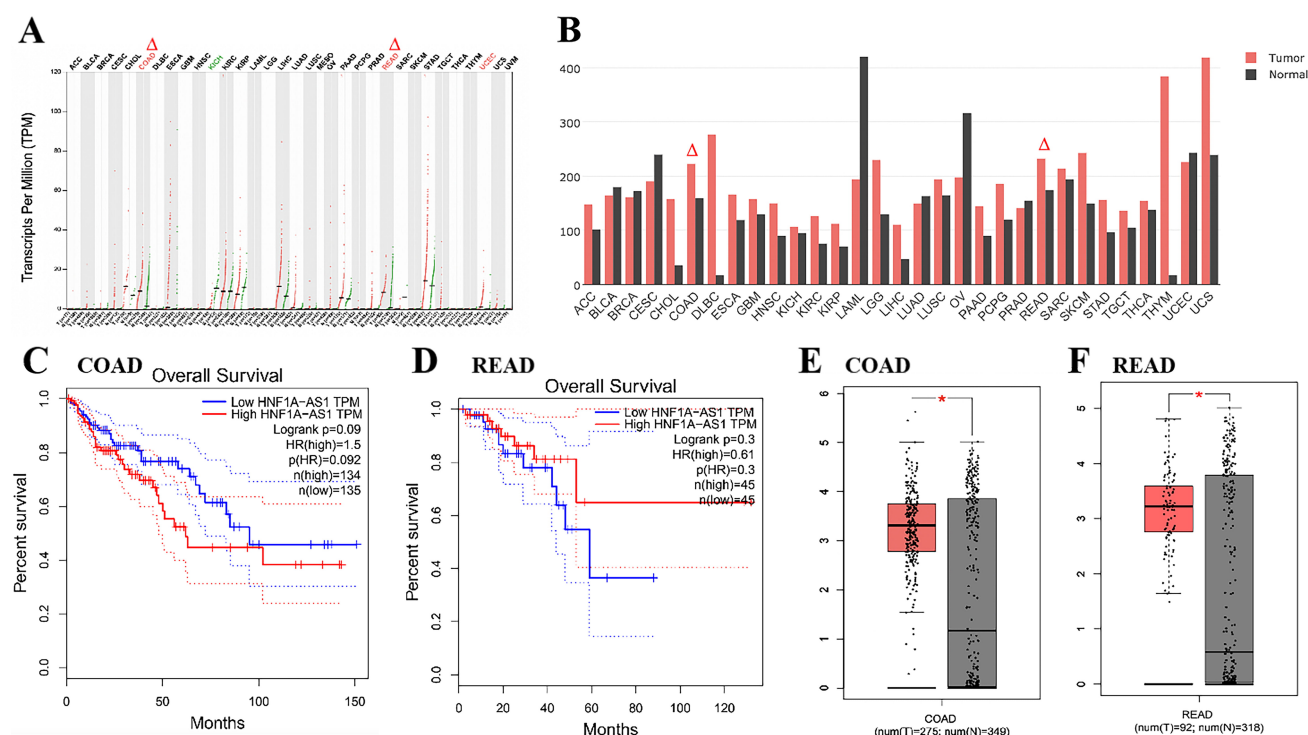
Fig. 1. LncRNA *HNF1A-AS1* is up-regulated and associated with OS. (A,B) The expression of *HNF1A-AS1* in disparate types of cancers were exhibited with red dots and in para-cancer is shown with green dots. Data derived from TCGA database portal in GEPIA. (B) The horizontal axis shows the type of tumor and the height of the bar represents the median expression of certain tumor types or normal tissue. (C) Kaplan-Meier analysis of colon cancer patients with high (n = 134) or low (n = 135) *HNF1A-AS1* levels. Statistical analysis was performed by log-rank test. (D) Kaplan-Meier analysis of rectal cancer patients with high (n = 45) or low (n = 45) *HNF1A-AS1* levels. Statistical analysis was performed by log-rank test. (E) The expression of *HNF1A-AS1* is up-regulated in colon cancer compared with para-cancer tissues (*$p < 0.05$). (F) The expression of *HNF1A-AS1* is up-regulated in rectal cancer compared with the para-cancer tissues (*$p < 0.05$). The triangle symbol highlights the two genes. The triangle symbol highlights the two tumor; OS,overall survival; COAD, colon adenocarcinoma; READ, rectum adenocarcinoma; HNF1A-AS1, LncRNA HNF1A antisense RNA 1.

3. Results

3.1 HNF1A-AS1 is Highly Expressed in Colon Cancer and Rectal Cancer Tissues Compared with Para-Cancer Tissues

GEPIA production plot analysis of LncRNA *HNF1A-AS1* gene expression in multiple cancer types and paired normal samples was performed, with each dot representing a different tumor or normal sample (Fig. 1A). It can be seen from the TCGA database that *HNF1A-AS1* is highly expressed in Colon adenocarcinoma (COAD) and Rectum adenocarcinoma (READ) (Fig. 1). The expression level of *HNF1A-AS1* in colon and rectal cancer is correlated with OS (Fig. 1C,D). In addition, we found that in the database of colon cancer and rectal cancer, *HNF1A-AS1* was highly expressed in cancer tissues compared with para-cancer tissues, and the difference was statistically significant ($p < 0.05$) (Fig. 1E,F).

3.2 HNF1A-AS1 Related miRNAs Analysis

The hierarchical cluster analysis showed that the expression of hnf1a-as1 target genes was different in 477

tumors and 41 neighboring tissues (Fig. 2A). Similarly, there were differences in the expression of 125 immune-related genes associated with *HNF1A-AS1* (Fig. 2B). With the cut-off |log2 (FoldChange)| ≥ 1 and p value < 0.05, compared with the control, we obtained 2027 up-regulated genes and 1404 down-regulated genes (Fig. 2C); In addition, based on TargetScan data, we found 65 miRNAs that may bind to *HNF1A-AS1* (Fig. 2D). GO and KEGG analysis of 125 genes are shown related to immunity including CD4-positive, alpha-beta T cell differentiation involved in immune response, T-helper 17 type immune response, T-helper 1 type immune response, the intestinal immune network for IgA production (Fig. 3A,B).

3.3 MiR-214 was Low Expressed in CRC Compared with Para-Cancer Tissues

RT-qPCR results demonstrated that compared with para-cancer tissues, *hsa-miR-1252-3p*, *hsa-miR-214*, *hsa-miR-3907*, *hsa-miR-4688-5p*, *hsa-miR-10527-5p* were less expressed ($p < 0.05$), while *HNF1A-AS1* was highly expressed in the CRC tissues ($p < 0.05$) (Fig. 4A). In addition, correlation analysis was conducted between *HNF1A-*
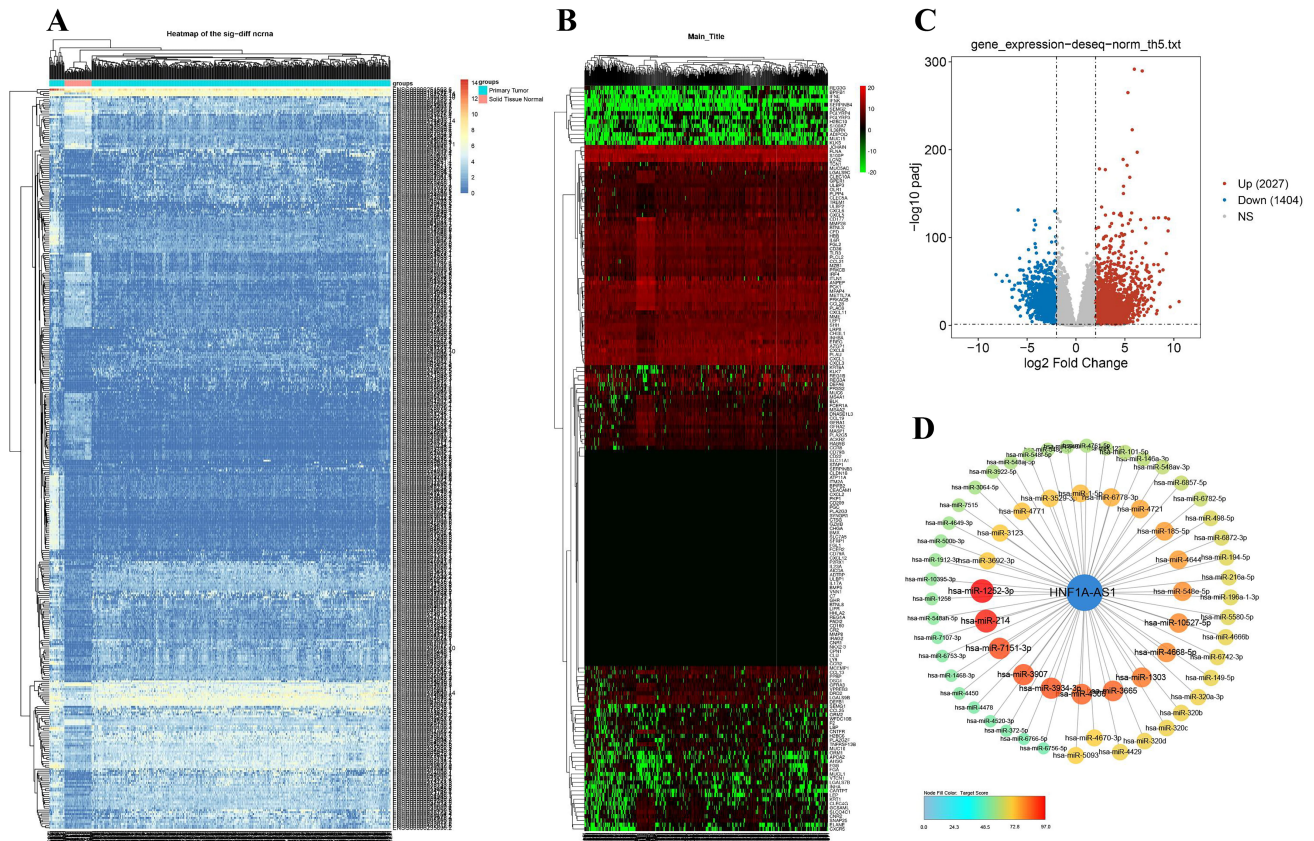
Fig. 2. The differential expression of *HNF1A-AS1* in tumor and adjacent tissues and its correlation with differential expression of miRNAs. (A) Hierarchical cluster analysis of *HNF1A-AS1* expression in 477 CRC and 41 adjacent tissues; The horizontal axis represents groups, and a black line represents a sample; The vertical axis represents the target gene of *HNF1A-AS1*. (B) Hierarchical cluster of 125 immune related gene expression differences associated with *HNF1A-AS1*; The e horizontal axis represents the grouping, and a black line represents a sample; The vertical axis shows 125 immune-related genes associated with *HNF1A-AS1*. (C) Volcano plot of differentially expressed miRNAs (DEMs). (D) Combined with TargetScan data, *HNF1A-AS1* potential associated with DEMs. CRC, colorectal cancer; DEMs, differentially expressed miRNAs

AS1 and the expression of *hsa-miR-1252-3p, hsa-miR-214, hsa-miR-3907, hsa-miR-4688-5p,* and *hsa-miR-10527-5p*. The results showed that *HNF1A-AS1* was negatively correlated with the expression of *hsa-miR-1252-3p, hsa-miR-214, hsa-miR-3907, hsa-miR-4688-5p* and *hsa-miR-10527-5p*. The expression of *HNF1A-AS1* was negatively correlated with that of *hsa-miR-214, hsa-miR-4688-5p* and *hsa-miR-1252-3p* ($p < 0.05$) (Fig. 4B,C,D,E,F).

3.4 The Target Gene INHBA of hsa-miR-214 is Highly Expressed in CRC

The miRDB, miRWalk, and TargetScan databases predicted four overlapping genes of *miR-214* target genes, namely *CXCR5, GFRA1, SNAP25* and *INHBA* (Fig. 5A). RT-qPCR results showed that compared with adjacent tissues, *CXCR5, GFRA1,* and *SNAP25* genes were less expressed in CRC, while *INHBA* gene was highly expressed in CRC ($p < 0.001$) (Fig. 5B–E).

3.5 MiRNA-214-5p is Positively Correlated with INHBA in Colon Cancer

The specific binding sites of INHBA-3'UTR and *miR-214-5p* were identified by starBase. The results indicated that *INHBA* might be the target gene of *miR-214-5p*, that is, *miR-214-5p* might regulate the expression of the *INHBA* gene through a post-transcriptional mode (Fig. 6A). Through enrichment analysis of the *INHBA* gene, it was found that *miR-214-5p* may be one of the key miRNAs regulated upstream from *INHBA* (Fig. 6B). Analysis of 450 colon cancer samples by TCGA database indicated that *miR-214-5p* is positively correlated with *INHBA* (Fig. 6C). The TCGA database was used to analyze the miRNAs data of 261 CRC tissues and normal control tissues. The results demonstrated that *miR-214-5p* was less expressed in tumor tissues compared with the adjacent tissues ($p < 0.01$) (Fig. 6D).
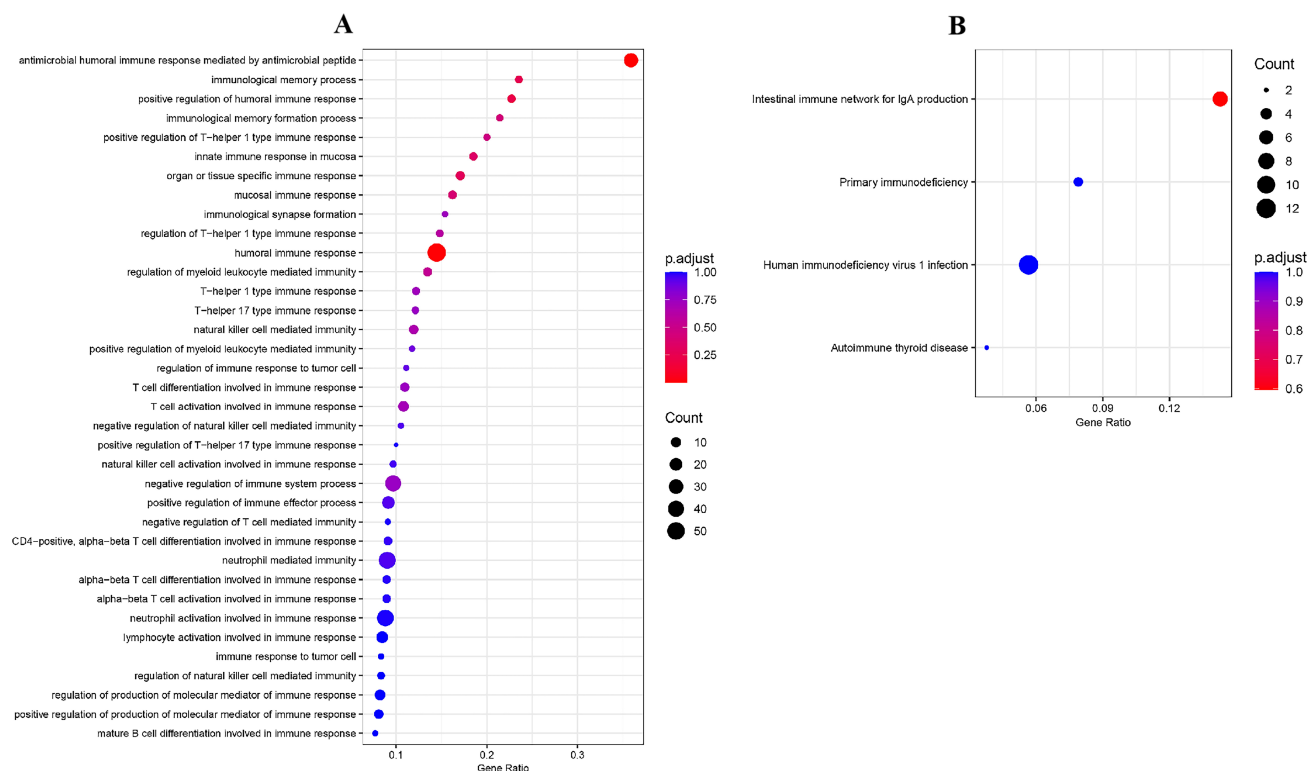
Fig. 3. GO annotation and KEGG pathway enrichment analysis. (A) A biological process rich in 125 genes related to immunity. (B) KEGG pathway enriched by 125 immune-related genes. GO, gene ontology; KEGG, Kyoto Encyclopedia of Genes and Genomes.
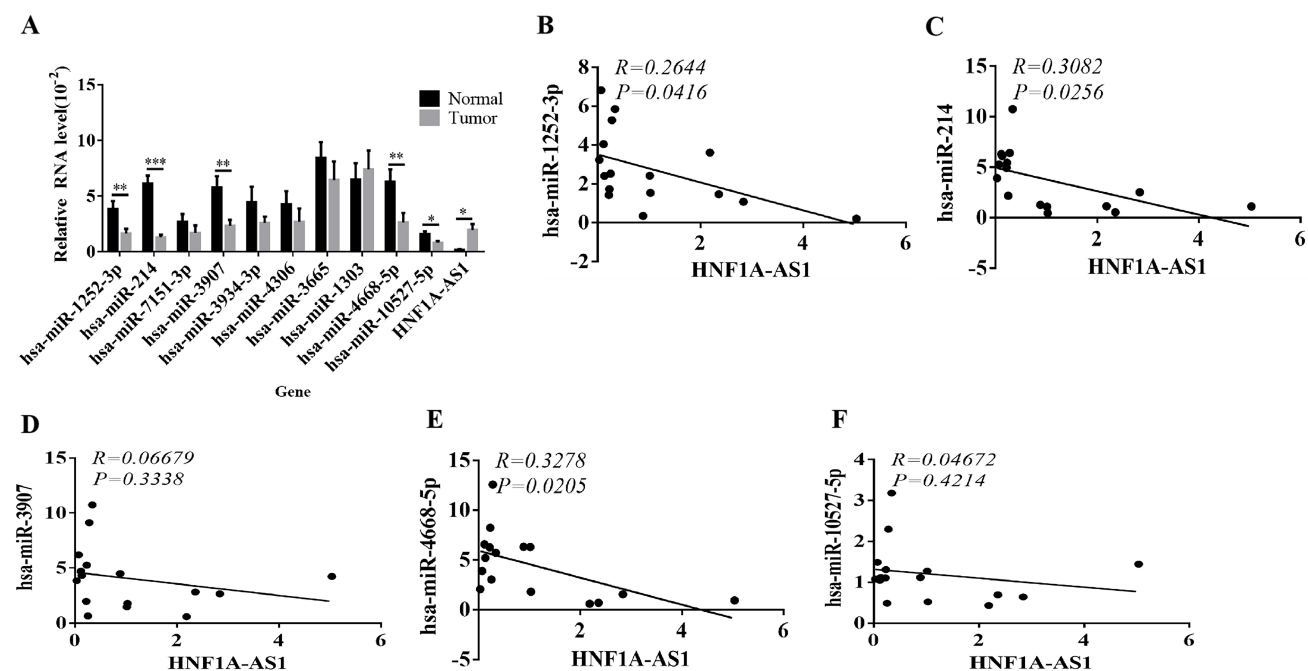

Fig. 4. Expression and correlation of *HNF1A-AS1* and related miRNAs. (A) mRNA expression of *HNF1A-AS1* and related miRNAs in tumor and normal tissues. (B) The correlation analysis between *hsa-miR-1252-3p* and *HNF1A-AS1* expression in CRC tissues. (C) The correlation analysis between *hsa-miR-214* and *HNF1A-AS1* expression in CRC tissues. (D) The correlation analysis between *hsa-miR-3907* and *HNF1A-AS1* expression in CRC tissues. (E) The correlation analysis between *hsa-miR-4668-5p* and *HNF1A-AS1* expression in CRC tissues. (F) The correlation analysis between *hsa-miR-10527-5p* and *HNF1A-AS1* expression in CRC tissues ($*p < 0.05$, $**p < 0.01$, $***p < 0.001$). R < 0.3, uncorrelated; $p < 0.05$, significant correlation.
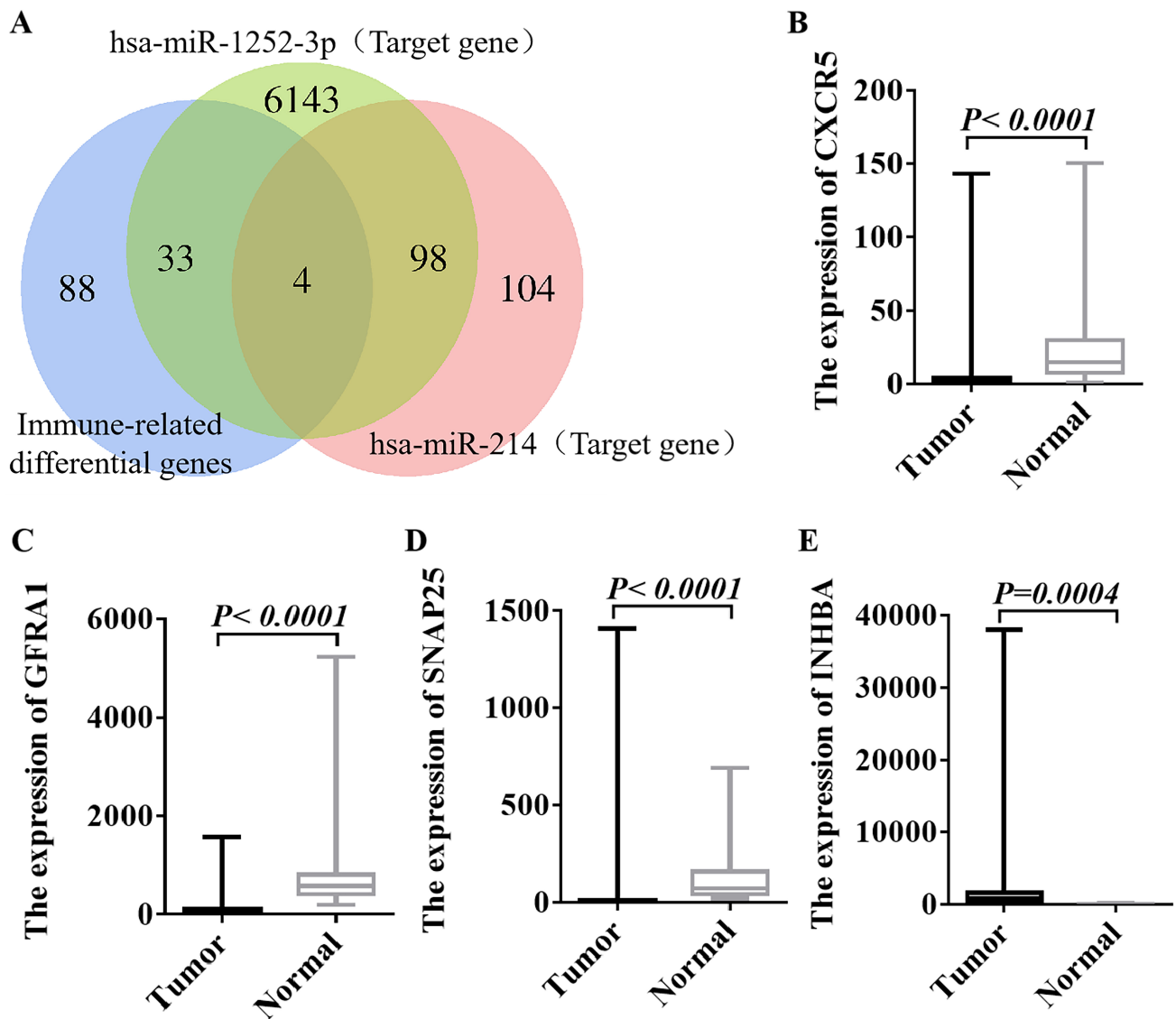
Fig. 5. Expression levels of target genes of *hsa-miR-214* in CRC (n = 10) and normal tissues (n = 10). (A) The miRDB, miRWalk, and TargetScan databases were utilized to predict the target genes of *hsa-miR-214*. (B) Expression of *CXCR5* gene in CRC and normal tissues. (C) Expression of *GFRA1* gene in CRC and normal tissues. (D) Expression of *SNAP25* gene in CRC and normal tissues. (E) Expression of *INHBA* gene in CRC and normal tissues. CXCR5, CXC ligand 5; GFRA1,GDNF family receptor α1; SNAP25 , synaptosome associated protein 25; INHBA, inhibin βA; $p < 0.05$, significant difference.

3.6 The Expression of INHBA Gene is Associated with the Progression of CRC

According to the transcriptome data of 473 CRC and 41 adjacent tissues gathered in the TCGA database, it was found that *INHBA* was highly expressed in cancer tissues (Fig. 7A,B), and the expression level of *INHBA* was positively correlated with the T stage of tumor, that is, the higher the expression level of *INHBA*, the later the T stage of patients ($p < 0.05$) (Fig. 7C). However, there was no correlation between the expression level of *INHBA* and the N stage, or M stage of the tumor ($p > 0.05$) (Fig. 7D,E). The survival curve analysis of the GEPIA database demonstrated that there was a negative correlation between the expression level of *INHBA* and the survival rate of CRC patients,

that is, the higher the expression level of *INHBA*, the lower the OS and DFS of CRC patients ($p < 0.05$) (Fig. 7F,G). A prognostic risk score model of CRC was constructed based on the *INHBA* gene, and the area under the curve (AUC) was: 0.996 (95% CI: 0.993–1.000, $p < 0.05$), indicating that the *INHBA* gene has high accuracy in predicting the prognosis of CRC (Fig. 7H).

3.7 INHBA is Highly Expressed in CRC Based on Experimental Verification

The expression level of *INHBA* was detected by the immunohistochemical method in 60 pairs of CRC tissues and adjacent tissues, and the positive rate was analyzed by Image-Pro Plus scanning software. Compared with para-
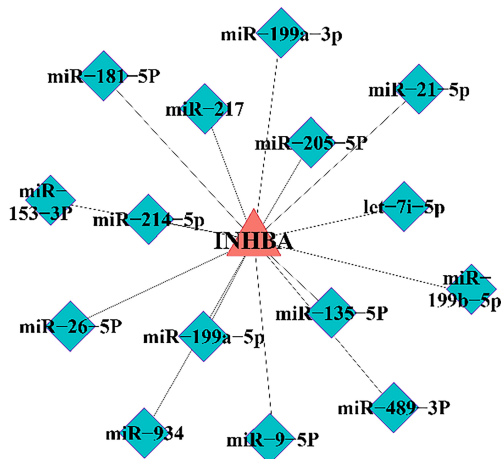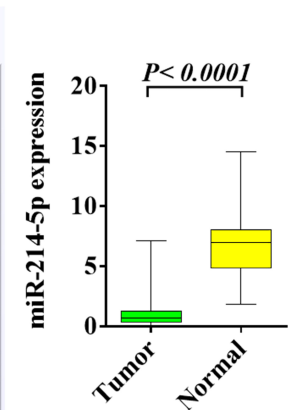
Fig. 6. Bioinformatics analysis of the upstream and downstream regulatory relationship between *miR-214-5p* and *INHBA* and their expression in CRC. (A) The binding site of *miRNA-214-5p* in *INHBA* was identified in the starBase. (B) The upstream and downstream regulatory relationship between *miRNA-214-5p* and *INHBA* was analyzed by enrichment. (C) *miRNA-214-5p* is positively correlated with *INHBA* in colon cancer patients based on TCGA database. (D) The expression of *miRNA-214-5p* in CRC and adjacent tissues was analyzed by TCGA database. $p < 0.05$, significant difference.

cancer tissues, the expression level of *INHBA* in CRC tissues was significantly up-regulated, with statistical significance ($p < 0.0001$) (Fig. 8A,D). RT-qPCR and Western Blot results indicated that the transcription and protein level of *INHBA* in CRC tissues were higher than those in adjacent tissues ($p < 0.05$) (Fig. 8B,C,E,F). In addition, *INHBA* was highly expressed in CRC cell lines (HT29, SW480 and SW620) compared with normal intestinal epithelial cells (NCM460) (Fig. 8G).

3.8 Transfection and Biological Capacity of HT29 and SW480 Cells

The proliferation and invasion abilities of HT29 cells in *HNF1A-AS1* shRNA ($p < 0.01$) and *INHBA* shRNA ($p < 0.01$) were both attenuated compared with those in the NC group (Fig. 9A,C), but the apoptosis was the opposite (Fig. 9E). The proliferation, invasion and apoptosis of SW480 cells in *HNF1A-AS1* shRNA ($p < 0.01$) and *IN-HBA* shRNA ($p < 0.01$) were similar to those of HT29 (Fig. 9B,D,F). This indicates that *HNF1A-AS1* and *INHBA* may be key target genes in CRC cell lines.

3.9 Patient Characteristics

A total of 60 pairs of tumor tissue samples from CRC patients meeting the inclusion and exclusion criteria were collected. The general baseline demographic and clinical data of patients are demonstrated in Table 2.

3.10 Relationship between Expression Level of INHBA and Clinicopathologic Features in CRC

χ^2 test was used to analyze the correlation between the expression of *INHBA* protein and the clinicopathologic characteristics of 60 CRC patients, such as age, gender, tumor size, degree of differentiation, depth of invasion (T stage), lymph node metastasis (N stage), distant metastasis (M stage), TNM stage, vascular invasion, nerve invasion, expression status of mismatch repair protein (MMR), and tumor location. The results showed that the expression of *INHBA* was significantly correlated with the degree of differentiation, depth of invasion, lymph node metastasis, distant metastasis, TNM stage, MMR status, and vascular invasion ($p < 0.05$), but was not significantly correlated with gender, age, tumor size, tumor location and nerve invasion ($p > 0.05$), as shown in Table 3.
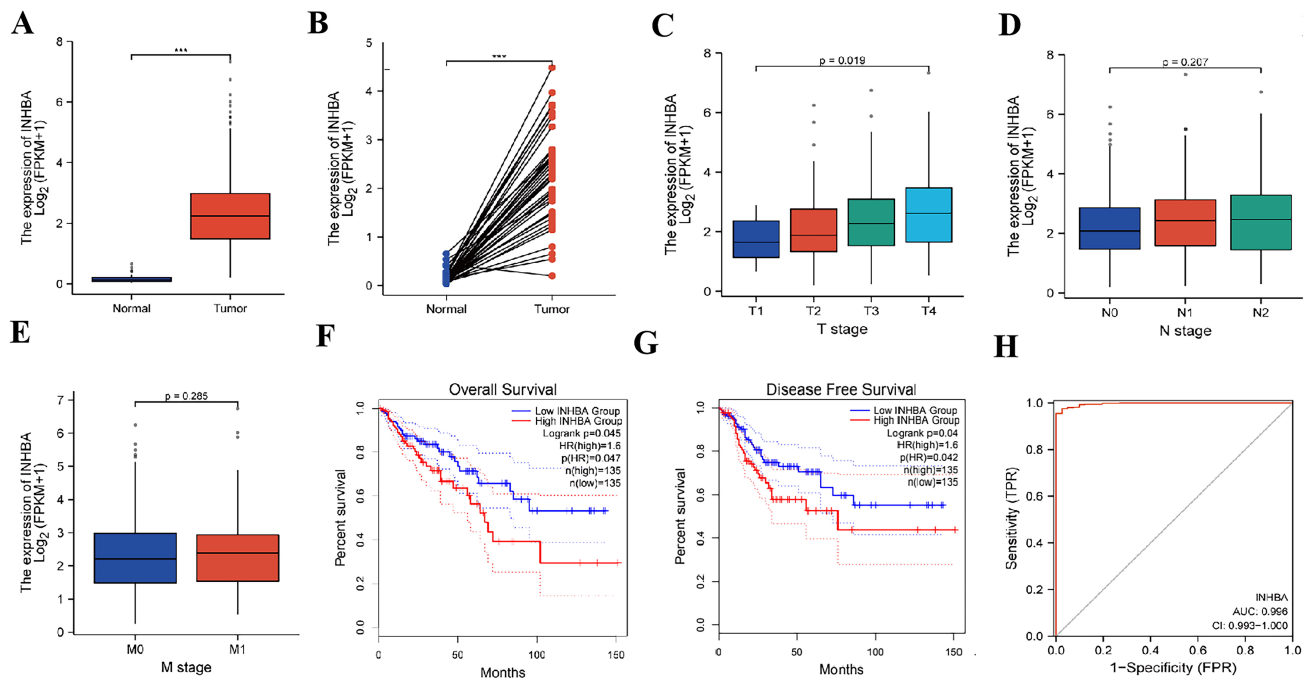
Fig. 7. Bioinformatics analysis of the expression of *INHBA* in CRC and its correlation with the prognosis. (A,B) The expression of *INHBA* in CRC and adjacent tissues was analyzed by TCGA database. (C) The expression of *INHBA* in different T stages of CRC was analyzed by TCGA database. (D) The expression of *INHBA* in different N stages of CRC was analyzed by TCGA database. (E) The expression of *INHBA* in different M stages of CRC was analyzed by TCGA database. (F) OS analysis corresponding to *INHBA* expression in CRC patients in GEPIA database. (G) DFS analysis corresponding to *INHBA* expression in CRC patients in GEPIA database. (H) Prognostic risk scoring model of CRC based on *INHBA* gene (***$p < 0.001$). DFS, Disease-free survival.
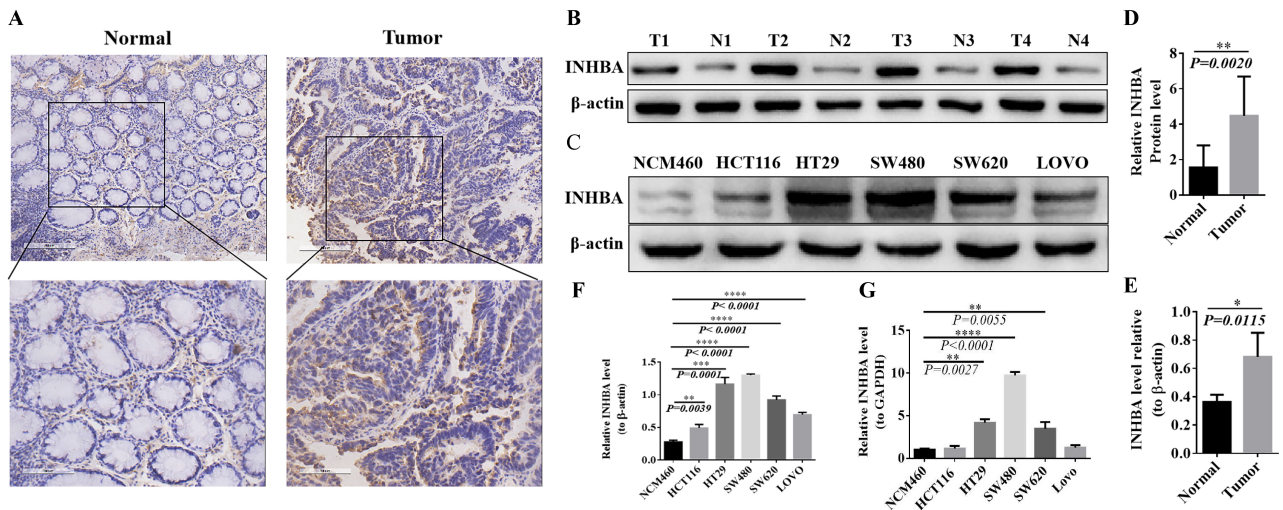

Fig. 8. Expression of *INHBA* in CRC tissues and cell lines. (A,B) Positive rate in normal and tumor tissues detection by IHC. (C,D) Expression levels in normal and tumor tissues detected by western blot. (E,F) Expression levels in CRC cell lines NCM460, HCT116, HT29, SW480, SW620 and LOVO detected by western blot. (G) mRNA expression levels in CRC cell lines NCM460, HCT116, HT29, SW480, SW620 and LOVO detected by qRT-PCR. The protein expression was normalized against β-actin, and mRNA expression was normalized for GAPDH. Expressed as relative expression ratio. (*$p < 0.05$, **$p < 0.01$, ***$p < 0.001$, ****$p < 0.0001$). IHC, immunohistochemical.

4. Discussion

Previous studies have shown that the *INHBA* gene can participate in the occurrence and development of gastric
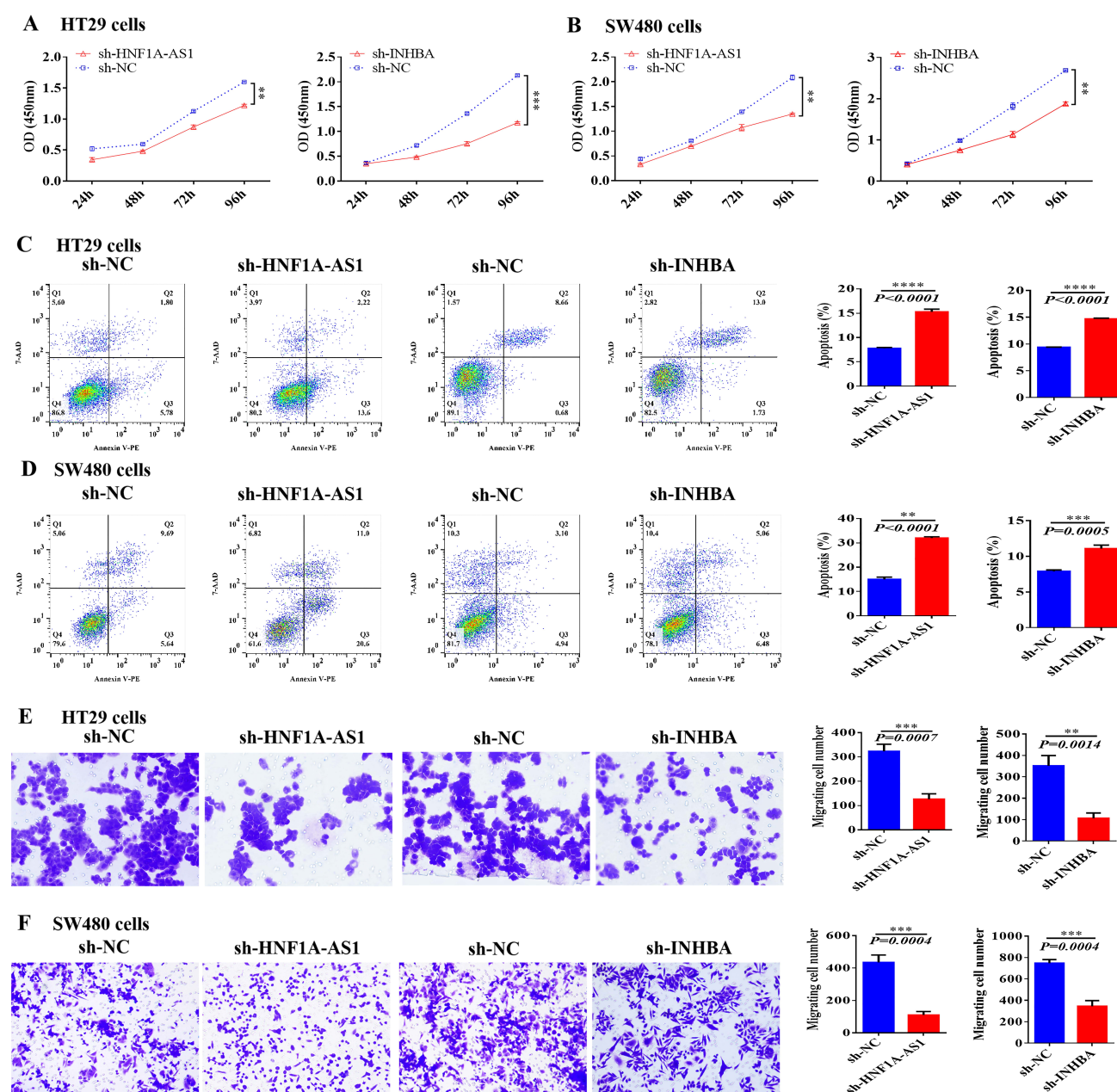
IMR Press

Fig. 9. Biological function of *HNF1A-AS1* and *INHBA* in human CRC cell lines. (A,B) HT29 and SW480 cells and their transfection with *HNF1A-AS1* shRNA and *INHBA* shRNA, respectively HT29 and SW480 cells and their transfection with *HNF1A-AS1* shRNA and *INHBA* shRNA, respectively proliferation at 24, 48, 72 and 96 h. (C,D) Apoptosis detection by flow cytometry. (E,F) Transwell invasion assay detects cell invasion ability (**$p < 0.01$, ***$p < 0.001$, ****$p < 0.0001$).

cancer by regulating the TGF-β/Smad signaling pathway [16]. It can also promote the invasion and metastasis of pancreatic cancer, breast cancer, hepatocellular carcinoma and non-small cell lung cancer by inducing EMT [17,18], promoting angiogenesis [14] and changing epigenetics [19]. The TGF-β/Smad signaling pathway is a tumor inhibitory pathway mediated by the membrane serine/threonine kinase receptor. Its main components include the TGF-β Superfamily, TGF-β Receptors, Smad Protein Family. Its nuclear transcription regulators and abnormalities in any component of this pathway can lead to tumorigenesis [20]. A recent study found that the knockdown of *INHBA* can significantly inhibit the expression of the TGF-β signaling pathway-related proteins in CRC cells [21].

However, the role of the *INHBA*-mediated TGF-β/Smad signaling axis in the development and progression of CRC remains to be further studied. The TCGA database was used to analyze the expression of *INHBA* in CRC and adjacent tissues, and the results demonstrated that *INHBA* was highly expressed in cancer tissues, and the expression level of *INHBA* was positively correlated with the T stage of tumor, that is, the higher the level of *INHBA*, the higher the

Table 2. The Baseline demographic and clinical characteristics of 60 CRC patients.

Clinical features		Sample size (n = 60)
Gender	Male	31
	female	29
Age (years)	≥50	50
	<50	10
Tumor size	≥3 cm	53
	<3 cm	7
Tumor differentiation	High	5
	Medium	28
	Low	27
Depth of invasion (T stage)	T1 + T2	18
	T3 + T4	42
Lymph node metastasis (N stage)	Yes	30
	No	30
Distant metastasis (M stage)	Yes	3
	No	57
TNM staging	I + II	28
	III + IV	32
Vascular infiltration	Yes	12
	No	48
Nerve invasion	Yes	6
	No	54
Tumor location	Right semicolon	21
	Left semicolon + rectum	39
Mismatch repair protein (MMR) status	dMMR	6
	pMMR	54

TNM, tumor node metastasis; dMMR, deficient mismatch repair; pMMR , proficient mismatch repair.

T stage of patients ($p < 0.05$). In order to verify the credibility of the database results, we collected clinical CRC tissue samples and tested the expression level of *INHBA* in the cancer tissue and the adjacent tissue by IHC, RT-qPCR and Western Blot respectively. The results of the three groups confirmed that the expression level of *INHBA* in the CRC tissues was significantly higher than that in the control adjacent tissue. In addition, compared with normal intestinal epithelial cells (NCM460), *INHBA* protein levels were highly expressed in CRC cell lines (HT29 and SW480). In addition, our study found that the higher the expression level of *INHBA* in CRC patient tumor tissues, the worse degree of differentiation, the higher T stage, N stage, and M stage, the more likely they are to develop vascular invasion, and to exhibit pMMR status. It was also found that there was no significant difference in the expression level of *INHBA* in either the right or left colon. Finally, survival curve analysis of the GEPIA database demonstrated that *INHBA* expression level was negatively correlated with OS and DFS in CRC patients. Therefore, we hypothesize that

INHBA, as a tumor suppressor gene, also promotes CRC progression by regulating the TGF-β/Smad signaling pathway, which will be further verified in subsequent studies.

Previous studies have confirmed that *miR-214* can play a tumor suppressive role in endometrial cancer, breast cancer and other tumors through diverse molecular mechanisms [22,23]. Studies also suggested that *miR-214* can be used as a crucial tumor suppressor in CRC [24]. For example, *miR-214* can inhibit the proliferation and metastasis of CRC by targeting the PLAGL2-MYH9 axis [25], while *miR-214* can also inhibit LIVIN and the NF-κB signaling pathway, which plays an anti-cancer role. Therefore, *miR-214* may inhibit the proliferation and metastasis of CRC. MiRNAs data of 261 colon cancer tissue samples and control samples collected from the TCGA database were analyzed, and the results showed that *miR-214* was less expressed in tumor tissues than in normal controls ($p < 0.01$). Other studies have found that *miR-214* can inhibit TGF-β mediated activation of pancreatic stellate cells and the occurrence of pancreatic cancer [26], but whether *miR-214* can inhibit the occurrence and development of CRC by down-regulating the activity of TGF-β/Smad signaling axis remains to be further verified. Bioinformatics enrichment analysis found that *miR-214* may be one of the key miRNAs regulated upstream of *INHBA*, and it was demonstrated that INHBA-3'UTR specifically binds to *miR-214*.

LncRNA has been proven to regulate various biological processes such as cell proliferation, apoptosis, invasion and metastasis, which provides a new perspective for the diagnosis and treatment of cancer [27]. *HNF1A-AS1* is highly expressed in diverse tumors, promoting the proliferation of triple-negative breast cancer [28], hepatocellular carcinoma [29] and glioma [30]; proliferation, migration and invasion of osteosarcoma [31]; proliferation, apoptosis, chemoresistance of non-small-cell cancer (NSCLC) [32]; proliferation, migration, EMT of oral squamous cell carcinoma [33]; invasion, metastasis, angiogenesis and lymphangiogenesis of gastric cancer [34]; metastasis and invasion of bladder cancer [35]; and proliferation, migration and invasion of esophageal adenocarcinoma [36]. Our results from TCGA database and clinical samples showed that *HNF1A-AS1* was highly expressed in CRC. In addition, there was a negative correlation between the expression of *HNF1A-AS1* and *miR-214* ($p < 0.05$).

5. Conclusions

In conclusion, our preliminary results suggest that the *HNF1A-AS1*/*miR-214*/*INHBA* axis regulates the TGF-β/Smad signaling pathway, which may be a potential mechanism affecting CRC. Subsequently, we will conduct detailed verification of the regulatory relationship between *HNF1A-AS1*/*miR-214*/*INHBA* axis at the cellular and animal levels. Meanwhile, *in vitro* and *in vivo* response experiments were conducted to demonstrate whether the *HNF1A-AS1*/*miR-214*/*INHBA* axis affects the development of CRC

Table 3. Relationship between INHBA expression level and clinicopathologic features of CRC.

Clinical features		Sample size (n = 60)	Expression level of INHBA		χ^2	p
			High expression	Lower expression		
Gender	Male	31	11	20	0.4746	0.6351
	Female	29	13	16		
Age (years)	≥50	50	20	30	0.3536	0.7237
	<50	10	4	6		
Tumor size	≥3 cm	53	21	32	0.2463	0.8055
	<3 cm	7	3	4		
Tumor differentiation	High	5	1	4		
	Medium	28	5	23	7.585	0.0225
	Low	27	14	13		
Depth of invasion (T stage)	T1 + T2	18	14	4	2.039	0.0415
	T3 + T4	42	19	23		
Lymph node metastasis (N stage)	Yes	30	7	23	2.635	0.0084
	No	30	17	13		
Distant metastasis (M stage)	Yes	3	0	3	1.965	0.0495
	No	57	33	24		
TNM staging	I + II	28	6	22	2.747	0.006
	III + IV	32	18	14		
Vascular infiltration	Yes	12	3	9	2.475	0.0133
	No	48	31	17		
Nerve invasion	Yes	6	1	5	1.151	0.2499
	No	54	22	32		
Tumor location	Right semicolon	21	9	12	1.115	0.2647
	Left semicolon + rectum	39	24	15		
Mismatch repair protein (MMR) status	dMMR	6	5	1	2.054	0.0400
	pMMR	54	20	34		

by regulating the TGF-β/Smad signaling pathway. Our results will provide new prognostic markers and therapeutic targets for CRC.

Availability of Data and Materials

Publicly available datasets were analyzed in this study. The datasets generated for this study can be found here: The Cancer Genome Atlas (TCGA) (https://portal.gdc.cancer.gov/), Gene Expression Profiling Anteractive Analysis (GEPIA) (http://gepia.cancer-pku.cn), miRDB(http://mirdb.org), miRWalk (http://mirwalk.umm.uni-heidelberg.de/), targetscan (http://www.targetscan.org/vert_80/), and starBase (https://ngdc.cncb.ac.cn/database commons/database/id/169#) databases.

Author Contributions

XZ, YL, TW, and RD were responsible for study design, data acquisition, and analysis and were major contributors to writing the manuscript. RQ, GL, YZ, XW, ZS, and RY helped to perform the mining of biological information and the data analysis. XC, YR, CD, and JL helped to perform the collection of specimens and experimental verification. All authors contributed to the article and approved the submitted version. All authors contributed to editorial changes in the manuscript. All authors read and approved the final manuscript. All authors have participated sufficiently in the work and agreed to be accountable for all aspects of the work.

Ethics Approval and Consent to Participate

The study protocols were approved by the Medical Institutional and Clinical Research Ethics Committee of Yunnan Cancer Hospital, the Third Affiliated Hospital of Kunming Medical University (Approval number: KYCS2022033). All experiments were carried out in accordance with the "Declaration of Helsinki" on the ethical principles for medical research involving human subjects. Written informed consent was obtained from all participants prior to their enrollment of the study.

Acknowledgment

Conflict of Interest

Supplementary Material

Supplementary material associated with this article can be found, in the online version, at https://doi.org/10.31083/j.fbl2811301.

References

[1] Bray F, Ferlay J, Soerjomataram I, Siegel RL, Torre LA, Jemal A. Global cancer statistics 2018: GLOBOCAN estimates of incidence and mortality worldwide for 36 cancers in 185 countries. CA: A Cancer Journal for Clinicians. 2018; 68: 394–424.

[2] Siegel RL, Miller KD, Fuchs HE, Jemal A. Cancer statistics, 2022. CA: A Cancer Journal for Clinicians. 2022; 72: 7–33.

[3] Xu F, Tang B, Jin TQ, Dai CL. Current status of surgical treatment of colorectal liver metastases. World Journal of Clinical Cases. 2018; 6: 716–734.

[4] Coppedè F, Lopomo A, Spisni R, Migliore L. Genetic and epigenetic biomarkers for diagnosis, prognosis and treatment of colorectal cancer. World Journal of Gastroenterology. 2014; 20: 943–956.

[5] Okugawa Y, Grady WM, Goel A. Epigenetic Alterations in Colorectal Cancer: Emerging Biomarkers. Gastroenterology. 2015; 149: 1204–1225.e12.

[6] Larsen KB, Lutterodt MC, Møllgård K, Møller M. Expression of the homeobox genes OTX2 and OTX1 in the early developing human brain. The Journal of Histochemistry and Cytochemistry. 2010; 58: 669–678.

[7] Omodei D, Acampora D, Russo F, De Filippi R, Severino V, Di Francia R, et al. Expression of the brain transcription factor OTX1 occurs in a subset of normal germinal-center B cells and in aggressive Non-Hodgkin Lymphoma. The American Journal of Pathology. 2009; 175: 2609–2617.

[8] Levantini E. Is miR therapeutic targeting still a miRage? Frontiers in Bioscience-Landmark. 2021; 26: 680–692.

[9] Zekri ARN, Youssef ASED, Lotfy MM, Gabr R, Ahmed OS, Nassar A, et al. Circulating Serum miRNAs as Diagnostic Markers for Colorectal Cancer. PLoS ONE. 2016; 11: e0154130.

[10] Evans JR, Feng FY, Chinnaiyan AM. The bright side of dark matter: lncRNAs in cancer. The Journal of Clinical Investigation. 2016; 126: 2775–2782.

[11] Huarte M. The emerging role of lncRNAs in cancer. Nature Medicine. 2015; 21: 1253–1261.

[12] Laird M, Glister C, Cheewasopit W, Satchell LS, Bicknell AB, Knight PG. 'Free' inhibin α subunit is expressed by bovine ovarian theca cells and its knockdown suppresses androgen production. Scientific Reports. 2019; 9: 19793.

[13] Shelling AN. Mutations in inhibin and activin genes associated with human disease. Molecular and Cellular Endocrinology. 2012; 359: 113–120.

[14] Singh P, Jenkins LM, Horst B, Alers V, Pradhan S, Kaur P, et al. Inhibin Is a Novel Paracrine Factor for Tumor Angiogenesis and Metastasis. Cancer Research. 2018; 78: 2978–2989.

[15] Chambers JC, Zhang W, Sehmi J, Li X, Wass MN, Van der Harst P, et al. Genome-wide association study identifies loci influencing concentrations of liver enzymes in plasma. Nature Genetics. 2011; 43: 1131–1138.

[16] Chen ZL, Qin L, Peng XB, Hu Y, Liu B. INHBA gene silencing inhibits gastric cancer cell migration and invasion by impeding activation of the TGF-β signaling pathway. Journal of Cellular Physiology. 2019; 234: 18065–18074.

[17] Deng S, Zhu S, Wang B, Li X, Liu Y, Qin Q, et al. Chronic pancreatitis and pancreatic cancer demonstrate active epithelial-mesenchymal transition profile, regulated by miR-217-SIRT1 pathway. Cancer Letters. 2014; 355: 184–191.

[18] Howley BV, Hussey GS, Link LA, Howe PH. Translational regulation of inhibin βA by TGFβ via the RNA-binding protein hnRNP E1 enhances the invasiveness of epithelial-to-mesenchymal transitioned cells. Oncogene. 2016; 35: 1725–1735.

[19] Seder CW, Hartojo W, Lin L, Silvers AL, Wang Z, Thomas DG, et al. Upregulated INHBA expression may promote cell proliferation and is associated with poor survival in lung adenocarcinoma. Neoplasia. 2009; 11: 388–396.

[20] Zhao M, Mishra L, Deng CX. The role of TGF-β/SMAD4 signaling in cancer. International Journal of Biological Sciences. 2018; 14: 111–123.

[21] He Z, Liang J, Wang B. Inhibin, beta A regulates the transforming growth factor-beta pathway to promote malignant biological behaviour in colorectal cancer. Cell Biochemistry and Function. 2021; 39: 258–266.

[22] Fang YY, Tan MR, Zhou J, Liang L, Liu XY, Zhao K, et al. miR-214-3p inhibits epithelial-to-mesenchymal transition and metastasis of endometrial cancer cells by targeting TWIST1. OncoTargets and Therapy. 2019; 12: 9449–9458.

[23] Han LC, Wang H, Niu FL, Yan JY, Cai HF. Effect miR-214-3p on proliferation and apoptosis of breast cancer cells by targeting survivin protein. European Review for Medical and Pharmacological Sciences. 2019; 23: 7469–7474.

[24] Han B, Ge Y, Cui J, Liu B. Down-regulation of lncRNA DNAJC3-AS1 inhibits colon cancer via regulating miR-214-3p/LIVIN axis. Bioengineered. 2020; 11: 524–535.

[25] Zhou Z, Wu L, Liu Z, Zhang X, Han S, Zhao N, et al. MicroRNA-214-3p targets the PLAGL2-MYH9 axis to suppress tumor proliferation and metastasis in human colorectal cancer. Aging. 2020; 12: 9633–9657.

[26] Kuninty PR, Bojmar L, Tjomsland V, Larsson M, Storm G, Östman A, et al. MicroRNA-199a and -214 as potential therapeutic targets in pancreatic stellate cells in pancreatic tumor. Oncotarget. 2016; 7: 16396–16408.

[27] Crea F, Clermont PL, Parolia A, Wang Y, Helgason CD. The non-coding transcriptome as a dynamic regulator of cancer metastasis. Cancer Metastasis Reviews. 2014; 33: 1–16.

[28] Yang J, Niu H, Chen X. GATA1-Activated HNF1A-AS1 Facilitates the Progression of Triple-Negative Breast Cancer via Sponging miR-32-5p to Upregulate RNF38. Cancer Management and Research. 2021; 13: 1357–1369.

[29] Wang C, Mou L, Chai HX, Wang F, Yin YZ, Zhang XY. Long non-coding RNA HNF1A-AS1 promotes hepatocellular carcinoma cell proliferation by repressing NKD1 and P21 expression. Biomedicine and Pharmacotherapy. 2017; 89: 926–932.

[30] Bi Y, Mao Y, Su Z, Du J, Ye L, Xu F. Long noncoding RNA HNF1A-AS1 regulates proliferation and apoptosis of glioma

IMR Press

through activation of the JNK signaling pathway via miR-363-3p/MAP2K4. Journal of Cellular Physiology. 2021; 236: 1068–1082.

[31] Lou P, Ding T, Zhan X. Long Noncoding RNA HNF1A-AS1 Regulates Osteosarcoma Advancement Through Modulating the miR-32-5p/HMGB1 Axis. Cancer Biotherapy & Radiopharmaceuticals. 2021; 36: 371–381.

[32] Wang Z, Liu L, Du Y, Mi Y, Wang L. The HNF1A-AS1/miR-92a-3p axis affects the radiosensitivity of non-small cell lung cancer by competitively regulating the JNK pathway. Cell Biology and Toxicology. 2021; 37: 715–729.

[33] Liu Z, Li H, Fan S, Lin H, Lian W. STAT3-induced upregulation of long noncoding RNA HNF1A-AS1 promotes the progression of oral squamous cell carcinoma via activating Notch signaling pathway. Cancer Biology & Therapy. 2019; 20: 444–453.

[34] Liu HT, Ma RR, Lv BB, Zhang H, Shi DB, Guo XY, et al. LncRNA-HNF1A-AS1 functions as a competing endogenous RNA to activate PI3K/AKT signalling pathway by sponging miR-30b-3p in gastric cancer. British Journal of Cancer. 2020; 122: 1825–1836.

[35] Feng Z, Wang B. Long non-coding RNA HNF1A-AS1 promotes cell viability and migration in human bladder cancer. Oncology Letters. 2018; 15: 4535–4540.

[36] Yang X, Song JH, Cheng Y, Wu W, Bhagat T, Yu Y, et al. Long non-coding RNA HNF1A-AS1 regulates proliferation and migration in oesophageal adenocarcinoma cells. Gut. 2014; 63: 881–890.